JOURNAL OF PETROLOGY | VOLUME 49 | NUMBER 11 | PAGES 1915–1929 | 2008 | doi:10.1093/petrology/egn047

Assessing Inheritance of Zircon and Monazite in Granitic Rocks from the Monashee Complex, Canadian Cordillera

J. L. CROWLEY[1]*, R. L. BROWN[2], F. GERVAIS[2] AND H. D. GIBSON[3]

[1]DEPARTMENT OF GEOSCIENCES, BOISE STATE UNIVERSITY, BOISE, ID 83725, USA

[2]DEPARTMENT OF EARTH SCIENCES, CARLETON UNIVERSITY, OTTAWA, ON, K1S 5B6, CANADA

[3]DEPARTMENT OF EARTH SCIENCES, SIMON FRASER UNIVERSITY, BURNABY, BC, V5A 1S6, CANADA

RECEIVED SEPTEMBER 5, 2007; ACCEPTED SEPTEMBER 10, 2008
ADVANCE ACCESS PUBLICATION NOVEMBER 7, 2008

Zircon and monazite from granitic sheets and dikes in the Monashee complex, Canadian Cordillera, were investigated to determine whether igneous crystallization occurred at 1·9 Ga or 50 Ma with 1·9 Ga inherited zircon and monazite. Four of the five samples are weakly deformed to undeformed, despite occurring in a gneiss dome at the structurally deepest exposed level of the orogen that elsewhere was strongly deformed and partly melted at 50 Ma. Based on U–(Th)–Pb ages from zircon and monazite, field relationships, and mineral composition and zoning, we conclude that the granitic rocks crystallized at 1·9 Ga and were metamorphosed at 50 Ma. All dated zircon is 1·9 Ga (except for 2·3–2·0 Ga inherited cores) and 1·9 Ga monazite makes up >90% of the population in four samples. The remainder of the monazite is 50 Ma and all monazite in one sample is 50 Ma. Composition and zoning of 1·9 Ga zircon and monazite are uniform within samples, yet differ between samples, indicating growth from 1·9 Ga magmas that are unique to each sample. This relationship is unlikely if the grains are inherited because the host rocks are heterogeneous 2·3–2·1 Ga gneisses. The 1·9 Ga zircon and monazite have zoning that is consistent with growth from magmas, whereas the 50 Ma monazite has variable composition and zoning that suggest growth from diverse metamorphic fluids. The results demonstrate that part of the Monashee complex was last strongly deformed and partly melted at 1·9 Ga, and thus largely escaped Cordilleran tectonism.

KEY WORDS: *Canadian Cordillera; inheritance; monazite; U–Pb geochronology; zircon*

INTRODUCTION

Crystallization ages of small-volume granitic rocks (e.g. dikes, sheets, veins, and pods of metaluminous to peraluminous granite, leucogranite, leucosome, and pegmatite) are crucial for constructing tectonic models of orogenic belts. Zircon and monazite are ideal for U–Pb dating of magma crystallization because of their moderate to high U concentrations and high closure temperature to diffusion of Pb (Harrison *et al.*, 2002; Parrish & Noble, 2003), yet close scrutiny is required before the ages can be accepted as ages of igneous crystallization because granitic rocks are notorious for containing inherited, xenocrystic zircon (e.g. Harrison *et al.*, 1987; Roddick & Bevier, 1995; Miller *et al.*, 2000; Bea *et al.*, 2007). Zircon from source and host rocks is not dissolved in magma that is saturated with respect to zircon, but rather is incorporated as partially resorbed xenocrysts. Zircon saturation is a function of bulk-rock chemistry, Zr concentration, and temperature of crystallization (Watson & Harrison, 1983). Small-volume granitic melts are usually produced by anatexis of peraluminous crustal rocks at temperatures low enough that complete zircon dissolution does not occur, and thus some degree of inheritance is expected in all melts. Inherited zircon varies from forming a minor part of the zircon population as rare cores within newly formed zircon to forming a large part as plentiful whole grains. Monazite saturation in granitic melts occurs in a similar way to zircon saturation (Rapp *et al.*, 1987; Montel, 1993),

*Corresponding author. Telephone: 208-407-8767. E-mail: jimcrowley@boisestate.edu

yet inherited monazite is rarely documented. The best known examples are two Himalayan leucogranites with sparse inherited monazite (Copeland *et al.*, 1988; Harrison *et al.*, 1995) and leucogranites in the Caledonides of East Greenland with plentiful inherited monazite (Gilotti & McClelland, 2005).

Discerning inherited from non-inherited zircon is central to some of the most intense geochronological debates, including that regarding the age of the oldest chemical evidence of life on Earth (Nutman *et al.*, 1997; Whitehouse *et al.*, 1999; Mojzsis & Harrison, 2002). Internal zoning patterns in zircon and Th/U of zircon were used to argue that the oldest parts are inherited and non-inherited, respectively. Interpretations of inheritance are often based on U–Pb ages alone. This approach is valid for zircon that is so old that inheritance is obvious. For example, inheritance is certain for Archean zircon in granite that intruded into Tertiary sedimentary rocks. However, inheritance cannot be proven by ages alone in granite lacking cross-cutting relationships because every zircon may be inherited. The composition and internal zoning patterns help identify inherited zircon, but inherited grains are difficult to identify when they formed in magma that is similar to the younger magma (e.g. zircon from peraluminous granite host rock that is inherited in peraluminous granite).

We assess inheritance in small-volume granitic bodies (meter-wide sheets and dikes of granite and pegmatite) in a gneiss dome in the metamorphic core of the Canadian Cordillera. A simple question prompted this study: did five granitic rocks crystallize at 1·9 Ga as part of the Laurentian basement or at 50 Ma as Cordilleran melts with 1·9 Ga inheritance? The crystallization ages have implications for Cordilleran tectonic models because intrusion of four of the samples occurred after the last penetrative ductile deformation and partial melting of the host gneisses. Our age interpretations are based on data from zircon and monazite, including U–(Th)–Pb ages obtained by laser ablation inductively coupled plasma mass spectrometry and electron microprobe, compositional data, internal zoning, and field relationships.

TECTONIC SETTING

A variety of models have been proposed for the tectonic evolution of the southeastern Canadian Cordillera that make contrasting assumptions about the ductility of adjacent gneiss domes in the deepest structural level, the Monashee complex (Fig. 1), during Tertiary orogenesis. Studies have proposed that the Thor–Odin dome (to the south) was hot and mobile whereas the Frenchman Cap dome (to the north) had parts that remained cool and solid. Tectonic models for the Thor–Odin dome include extension-assisted diapirism (Vanderhaeghe *et al.*, 1999), flow of ductile middle crust toward a rolling hinge during extension (Teyssier *et al.*, 2005), and channel flow (Williams & Jiang, 2005) or extrusion (Johnston *et al.*, 2000) during compression. Models for the Frenchman Cap dome (Fig. 2) include basement duplexing (Brown *et al.*, 1986; Journeay, 1986), underthrusting of relatively cold basement (Parrish, 1995; Crowley *et al.*, 2001), and basement being the base of a channel flow (Brown & Gibson, 2006).

Critical to the tectonic models is the age of granitic rocks (granite, leucogranite, leucosome, and pegmatite that occur as dikes, sheets, veins, and pods). Leucosomes in migmatites in the Thor–Odin dome with ~55 Ma zircon rims around cores show Tertiary igneous crystallization and Paleoproterozoic inheritance (Vanderhaeghe *et al.*, 1999; Hinchey *et al.*, 2006). In contrast, granitic rocks in the northern part of the Frenchman Cap dome have mostly 1·9 Ga zircon and monazite that were interpreted as forming during igneous crystallization (Armstrong *et al.*, 1991; Crowley, 1999). However, because dating of the Frenchman Cap dome samples was performed on single- and multi-grain analyses by the isotope dilution thermal ionization mass spectrometry (ID-TIMS) method without knowledge of the internal zoning of the grains, it cannot be ruled out that the 1·9 Ga grains are inherited in Tertiary granitic rocks. If this alternative hypothesis is true, there would be no evidence for basement remaining rigid through the Tertiary. The purpose of our study is to re-examine the age of granitic rocks in the Frenchman Cap dome by using *in situ* methods.

The Frenchman Cap dome is mostly composed of Paleoproterozoic gneisses that are layered at the meter scale (Journeay, 1986). The dominant orthogneiss in the study area is 2·08 Ga K-feldspar augen granitic gneiss (Crowley, 1999). Other important units are ~2·1 Ga granitic orthogneiss and ~2·3 Ga dioritic gneiss (Crowley, 1999). Paragneiss units derived from sedimentary and volcanic rocks are presumed to be older than the orthogneiss units. Monazite in the paragneiss grew at 2·1 Ga and 50 Ma (Crowley & Parrish, 1999). Younger gneisses are known from outside the study area, including 1·86 Ga granodioritic orthogneiss 30 km to the NW (Crowley, 1997), and 1·93 Ga granodioritic augen orthogneiss and ~1·87 Ga homogeneous granitic gneiss in the Thor–Odin dome (Parkinson, 1991).

ANALYTICAL METHODS

Five granitic rocks were collected at Bourne Glacier, Monashee Mountains, British Columbia (Fig. 2; UTM coordinates are given in Electronic Appendix 1, which is available for downloading at http://www.petrology.oxfordjournals.org). Zircon and monazite were isolated using standard mineral separation techniques, mounted in epoxy, and polished to reveal the centers. Cathodoluminescence (CL) images of the polished zircon and backscattered electron (BSE) images of the polished monazite were

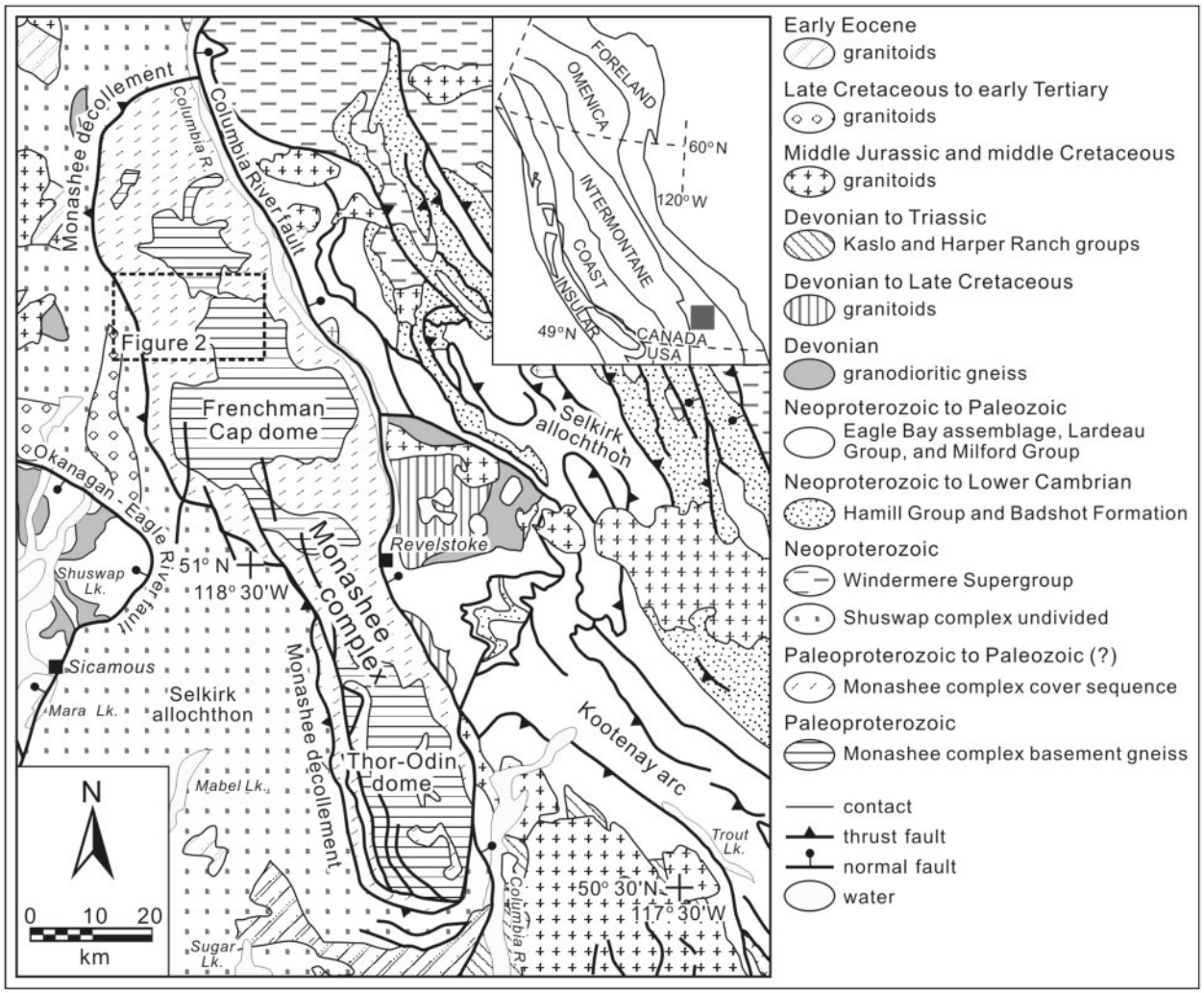

Fig. 1. Tectonic assemblage map in the vicinity of the Monashee complex, modified after Wheeler & McFeely (1991), showing the location of Fig. 2. The dark grey square in inset locates the map with respect to the morphogeological belts of the Canadian Cordillera.

acquired using a JEOL JXA-733 Superprobe at the Massachusetts Institute of Technology. Elemental compositions of polished monazite were measured by electron probe microanalysis (EPMA) with an accelerating voltage of 15 kV and beam current of 100 nA. Counting times on peak were 120 s for Pb, 60 s for U and Y, and 20 s for all other elements. Counting time on backgrounds were the same and split between each side of the peak. Background positions were carefully chosen to avoid secondary peak interferences and the detectors were optimally set for pulse-height analysis. UMβ was used for U measurement and the intensity was corrected for Th interference. PbMα was measured and its intensity was corrected for Y and Th interferences. Lβ X-rays were used to measure Nd, Pr, Gd and Sm. Interferences among the rare earth elements were corrected as outlined by Pyle *et al.* (2002). Interference correction in the X-ray intensity of an element was based on the intensity of the same X-ray in a standard free of that element but containing the interfering element. For example, UMβ intensity in the sample was corrected for Th interference by subtracting the UMβ intensity in U-free thorite (the Th standard) multiplied by the *k*-ratio of ThMα in the sample. Raw data were corrected for matrix effects with the CITZAF program (Armstrong, 1995). Data are given in Electronic Appendix 2.

Chemical U–Th–Pb ages based on concentrations from EPMA were calculated to guide dating by laser ablation inductively coupled plasma mass spectrometry (LA-ICPMS) and estimate the age of domains that are too small for LA-ICPMS dating. Because a low degree of accuracy and precision was required to distinguish between monazite that is Paleoproterozoic (thousands of ppm Pb) from that which is Tertiary (zero to hundreds of ppm Pb), the U, Th, and Pb measurements were made relatively

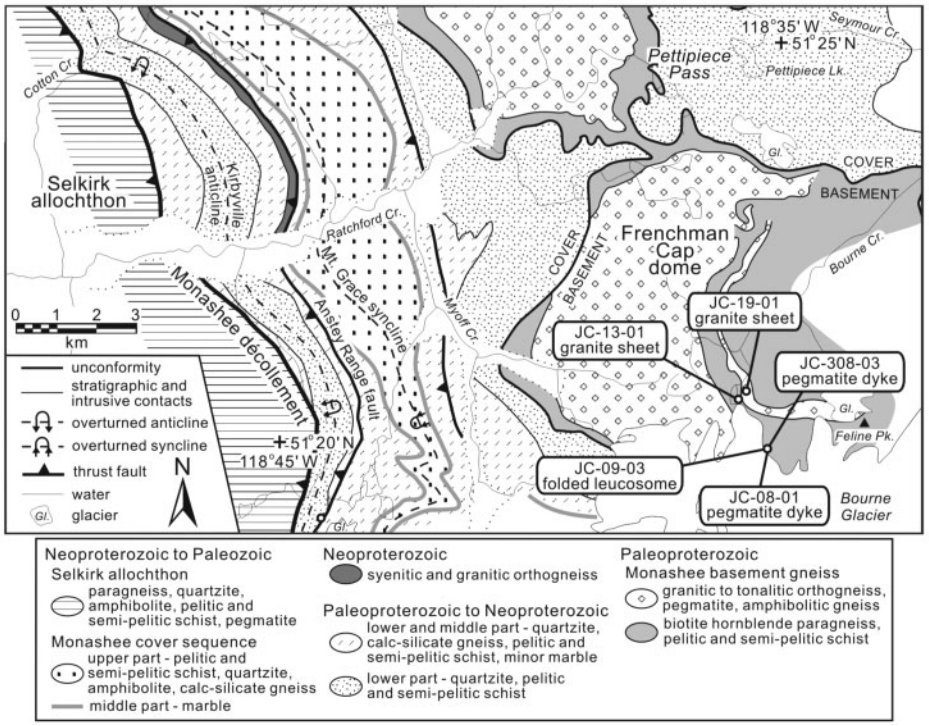

Fig. 2. Geological map of the northern part of the Frenchman Cap dome, modified after Wheeler (1965) and Journeay (1986), showing sample localities.

quickly and thus the ages are considered to be reconnaissance. Accuracy of the U–Th–Pb chemical ages was confirmed by the LA-ICPMS dating that showed Paleoproterozoic and Tertiary chemical ages were from 1·9 Ga and 50 Ma monazite, respectively. Identification of domains in several monazite grains was facilitated with X-ray maps of Pb, Th, U, and Y made by EPMA on a Cameca SX-50 at the University of Massachusetts (Goncalves *et al.*, 2005). In particular, the approximate age of the domains (Paleoproterozoic vs Tertiary) was discerned from the X-ray maps of Pb.

U–Pb isotopic measurements of zircon and monazite were performed by ICPMS using a VG PlasmaQuad PQ-2S+ system attached to an in-house built 266 nm frequency coupled Nd–YAG laser ablation (LA) microprobe at Memorial University of Newfoundland (Jackson *et al.*, 1992). The LA-ICPMS dating method broadly followed that outlined by Košler & Sylvester (2003) and Crowley *et al.* (2005). The laser produced an ~38 and ~25 μm wide square pit in zircon and monazite, respectively, by rastering the stage beneath the laser beam. The pit was ~10 μm deep. The efficiency of the mass bias correction and a correction for laser-induced fractionation were monitored by measurements of the zircon standard 91500 (Wiedenbeck *et al.*, 1995) and an in-house ~550 Ma monazite standard from Madagascar after every seven analyses of unknowns. U–Pb concordia plots and histograms in Fig. 3 were constructed with Isoplot (Ludwig, 2003) based on data in Electronic Appendix 1. Paleoproterozoic ages are given as $^{207}Pb/^{206}Pb$ ages and Tertiary ages are given as $^{206}Pb/^{238}U$ ages. Errors are 2σ.

RESULTS

JC-09-03 (folded pegmatite)

Sample JC-09-03 is from a narrow (up to 0·5 m wide) pegmatite layer showing pinch-and-swell. It was deformed by two phases of folding (Fig. 4a): the earlier phase was tight and axial planar to the dominant gneissosity in the host gneisses and the later phase was upright and open. Although it is uncertain whether the folded pegmatite underwent all deformation experienced by the host gneisses, it was clearly more deformed than the other samples, including JC-08-03 and JC-308-03 from the same outcrop.

Zircon is composite with oscillatory-zoned CL-dark rims around CL-bright cores with zoning that is truncated at the boundary with the rims (Fig. 5a). The U-rich nature of the rims is indicated by the CL-dark character that is typical of zircon with high U concentrations. Zircon ages from the rims are concordant to highly discordant. The array on the concordia plot indicates that the disturbance to the system occurred relatively recently, probably as a result of Pb loss in these U-rich grains, and thus the $^{207}Pb/^{206}Pb$ ages should be close to the primary ages. Sixteen ages (from 13 grains)

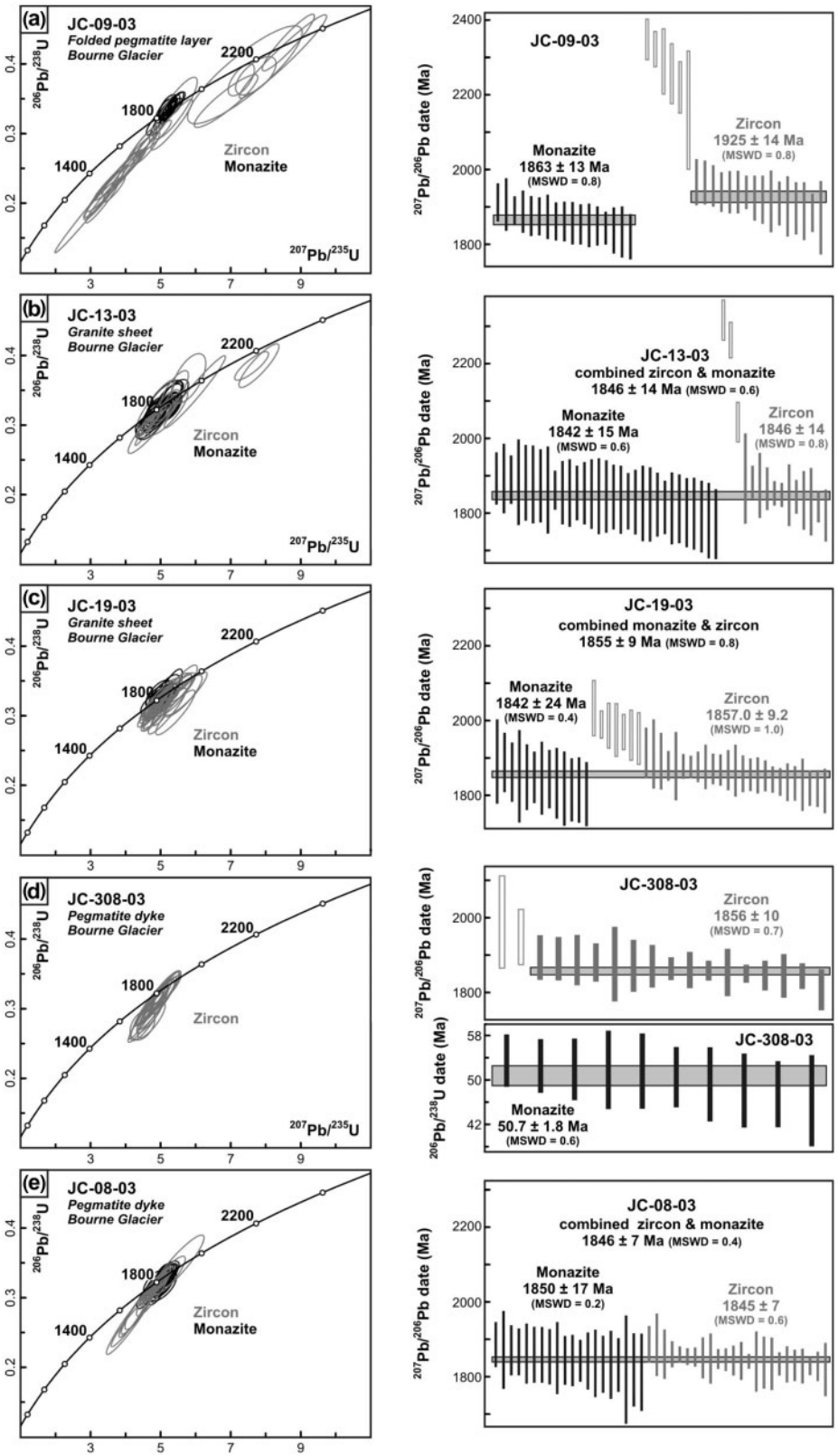

Fig. 3. U–Pb concordia plots and histograms of LA-ICPMS $^{207}Pb/^{206}Pb$ and $^{206}Pb/^{238}U$ ages. Long grey bars in histogram show the weighted mean age. Unfilled age bars were not used in the weighted mean calculations because they are from zircon interpreted as being inherited. Errors are 2σ.

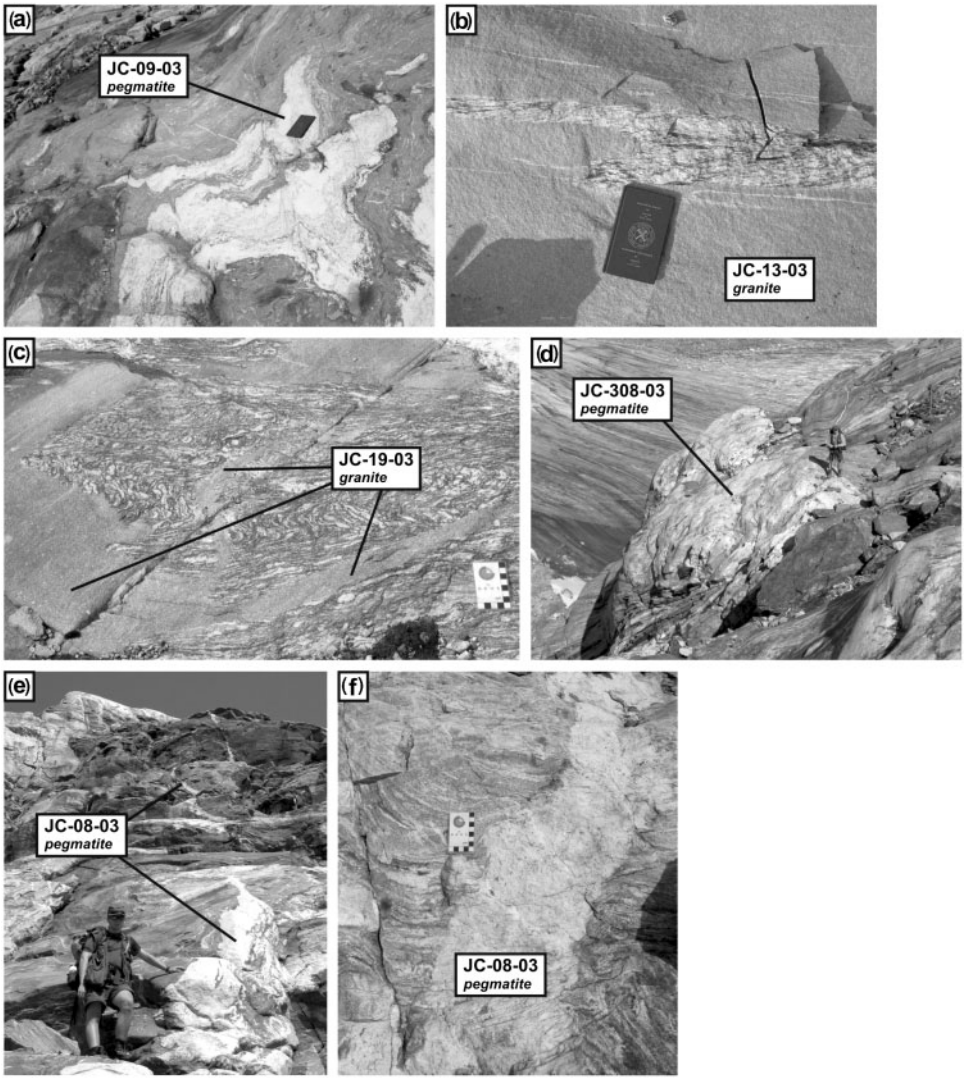

Fig. 4. Field relationships of dated samples. Notebook is 20 cm long and card is 8 cm long. (a) JC-09-03 is from a pegmatite layer that was deformed by two generations of folds. Sample was collected 2 m from this locality. (b) JC-13-03 is from a granite sheet that is homogeneous and weakly deformed where it cuts across gneissosity in the host gneiss (above notebook). Sample was collected 3 m from this locality. (c) JC-19-03 is from a granite sheet that is homogeneous and weakly deformed where narrow apophyses cut across gneissosity in host gneiss. Sample was collected ~10 m from this locality. (d) JC-308-03 is from a vertical pegmatite dike that cuts gneissosity in host gneiss at a high angle. Sample was collected below geologist. (e) JC-08-03 is from a narrow, vertical pegmatite dike that cuts gneissosity in host gneiss at a high angle. Sample was collected part-way up the outcrop. (f) JC-08-03 pegmatite dike cuts gneissosity in host gneiss at a high angle. Locality is several meters below outcrop shown in photograph (e).

from the CL-dark rims yielded a weighted mean age of 1925 ± 15 Ma (MSWD = 0·8) (Fig. 3a). Six CL-bright cores have ages of 2·3–2·2 Ga. Monazite has weak patchy zoning (Fig. 6a). Seventeen grains yielded a weighted mean age of 1863 ± 13 Ma (MSWD = 0·8) (Fig. 3a). Monazite has domains that appear to have formed by recrystallization of the weak patchy-zoned monazite because of their irregular shapes (Fig. 6a). EPMA dating (Fig. 6a) and X-ray mapping (Fig. 7a) show that the secondary monazite is more commonly Tertiary than Paleoproterozoic. Three LA-ICPMS ages from secondary monazite yielded a weighted mean age of 46·8 ± 2·0 Ma (MSWD = 0·7), with one grain being entirely Tertiary. Tertiary monazite is more compositionally diverse than Paleoproterozoic monazite, and is relatively U- and Ca-depleted and Si-enriched (Figs 7a and 8).

JC-13-03 (granite sheet)

Sample JC-13-03 is from a sheet of grey medium-grained biotite granite of several meters width (Fig. 4b) that is interpreted as being part of the Bourne granite suite that pervasively intruded the basement orthogneiss in the northern part of the dome (Crowley, 1999). The ubiquity,

Fig. 5. CL images of zircon, showing location of LA-ICPMS spots with ^{207}Pb/^{206}Pb ages.

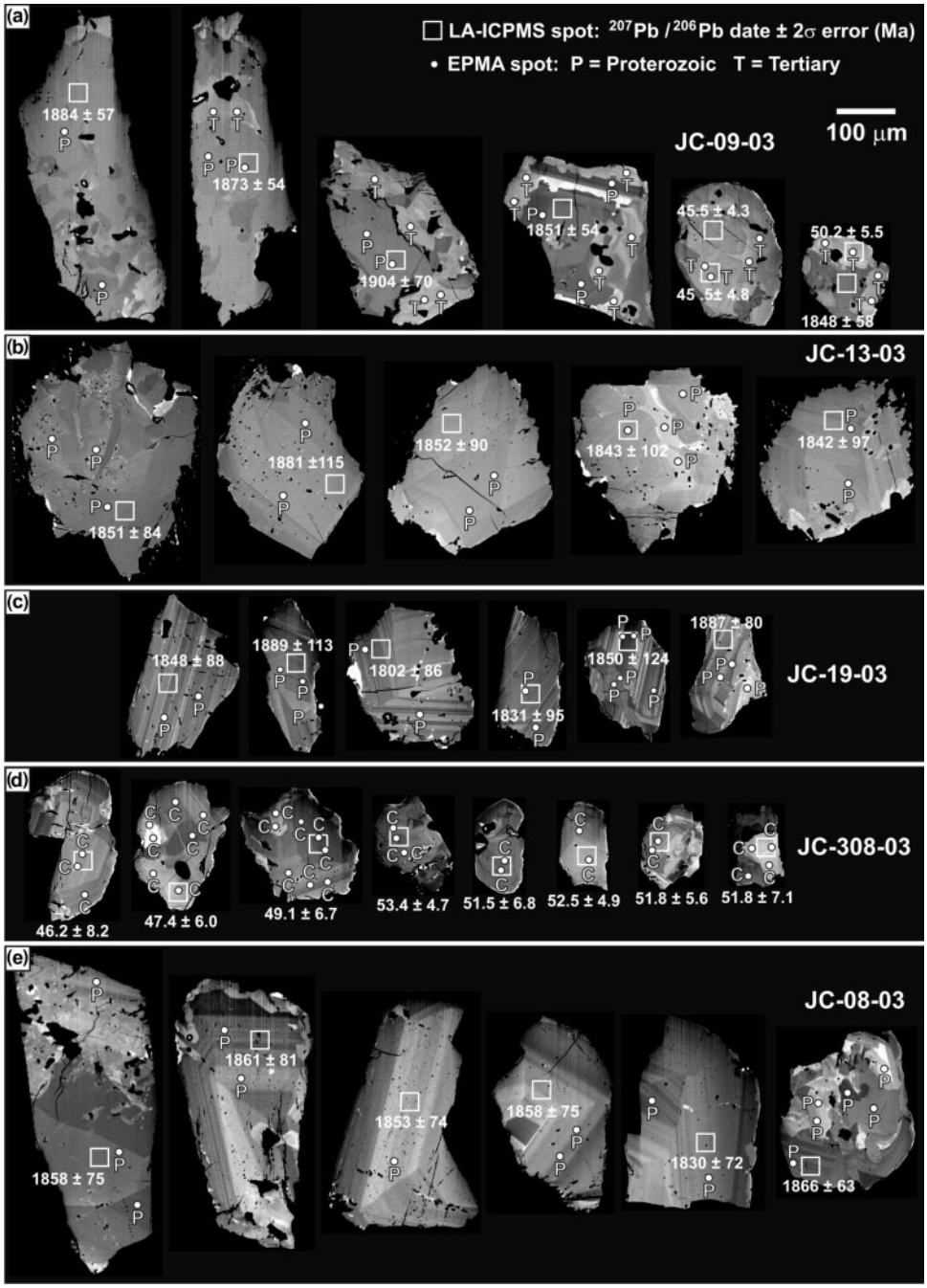

Fig. 6. BSE images of monazite, showing location of LA-ICPMS spots with $^{207}Pb/^{206}Pb$ and $^{206}Pb/^{238}U$ ages and EPMA spots with reconnaissance U–Th–Pb ages.

characteristic appearance, and intrusive relationships of Bourne granite make it the most valuable strain marker in the region. The sheet has a homogeneous and equigranular texture, with weak lineation and foliation. The near-pristine appearance of the granite, including where it is highly discordant to the gneissosity in the host augen gneiss (Fig. 4b), indicates that intrusion postdated migmatization.

Zircon is mostly oscillatory- and sector-zoned (Fig. 5b). Twelve grains yielded a weighted mean age of 1846 ± 14 Ma (MSWD = 0·8) (Fig. 3b). Oscillatory- and sector-zoned zircon is typically surrounded by CL-dark rims (Fig. 5b) that are too narrow (<20 mm wide) for dating with the laser pit size used in this study. Cores and whole grains with different zoning patterns and CL brightness are common, with three grains having ages of

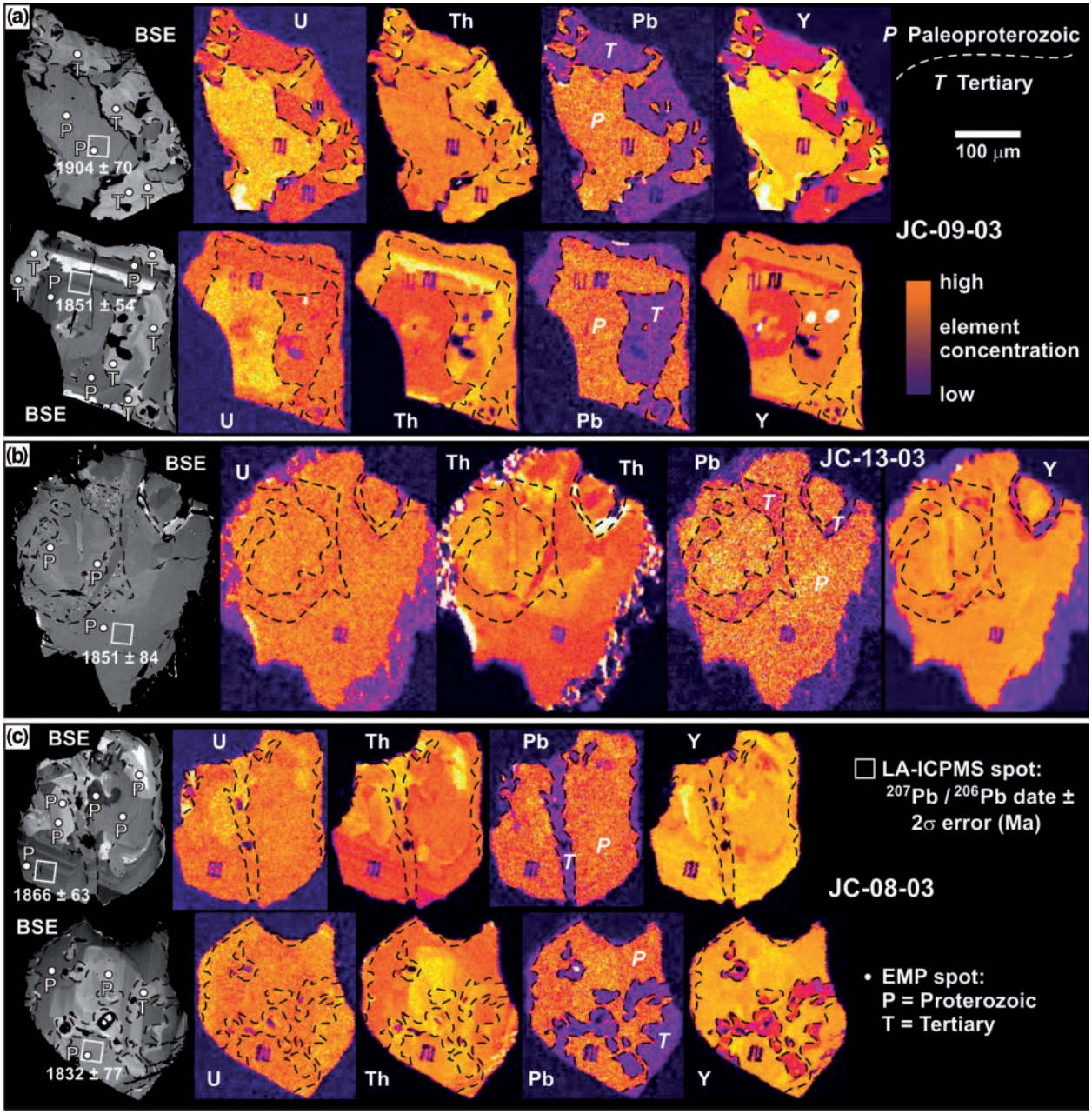

Fig. 7. Maps of U, Th, Pb, and Y in monazite obtained by EPMA. BSE images at left show location of LA-ICPMS spots with $^{207}Pb/^{206}Pb$ ages and EPMA spots with reconnaissance U–Th–Pb ages. Dashed line is the boundary between Paleoproterozoic and Tertiary monazite indicated by the Pb map.

2·3–2·0 Ga. Monazite is moderately sector-zoned (Fig. 6b) and commonly surrounded by thick (hundreds of microns wide) coronas resulting from the breakdown of monazite to (in order of decreasing abundance) apatite, allanite, Th-rich monazite, phengite, and thorite. Thirty-one grains yielded a weighted mean age of 1842 ± 15 Ma (MSWD = 0·6) (Fig. 3b). The combined zircon and monazite weighted mean age is 1846 ± 14 Ma (MSWD = 0·6). Monazite has small (a few microns) to medium-sized (50 μm) domains that are interpreted as having formed by recrystallization of the sector-zoned monazite because of their irregular shapes and truncation of primary zoning (Fig. 6b). EPMA dating (Fig. 6b) and X-ray mapping (Fig. 7b) show that Paleoproterozoic secondary domains are larger and more common than Tertiary domains. Paleoproterozoic secondary monazite is compositionally similar to primary monazite (Fig. 8) and Tertiary monazite is Y-poorer (Fig. 7b).

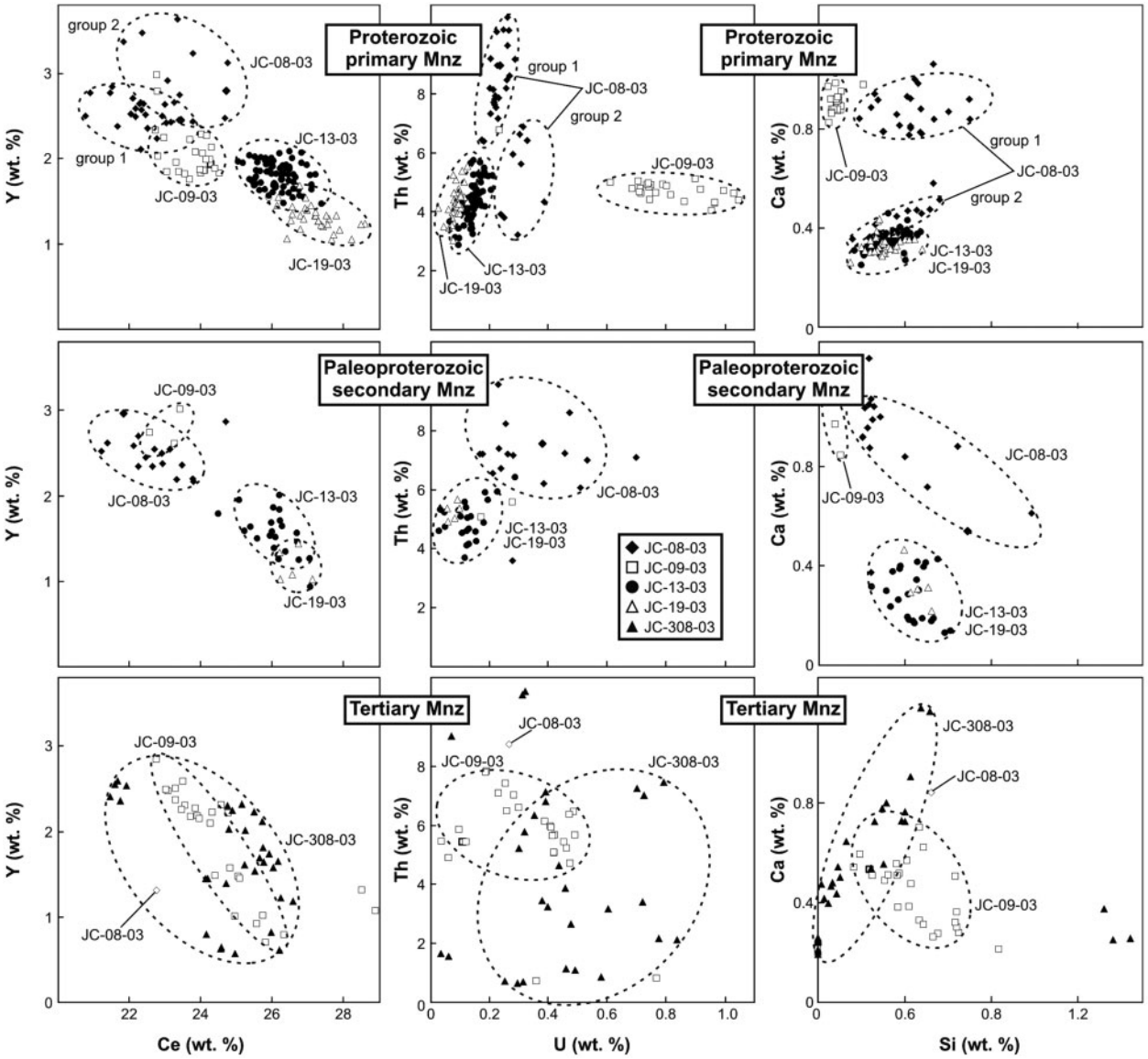

Fig. 8. Plots of element concentrations in monazite obtained by EPMA.

JC-19-03 (granite sheet)

Sample JC-19-03 is from a meter-wide sheet of grey medium-grained biotite granite with centimeter-wide apophyses that cut across the gneissosity in the host gneiss at high angles (Fig. 4c). It is similar to JC-13-03 and considered as being part of the Bourne granite suite.

Zircon is oscillatory- and sector-zoned (Fig. 5c). Twenty-five grains yielded a weighted mean age of 1857 ± 9 Ma (MSWD = 1·0) (Fig. 3c). Cores with different zoning patterns and CL brightness are common. Seven cores yielded a weighted mean age of 1980 ± 21 Ma (MSWD = 0·6). Monazite is strongly oscillatory-zoned (Fig. 6c) and has coronas similar to those in sample JC-13-03. Thirteen grains yielded a weighted mean age of 1842 ± 24 Ma (MSWD = 0·4) (Fig. 3c). The combined zircon and monazite weighted mean age is 1855 ± 9 Ma (MSWD = 0·8). Some monazite grains have small- (a few microns) to medium-sized (50 μm) domains that are interpreted as having formed by recrystallization because of their irregular shapes and truncation of primary zoning (Fig. 6c). EPMA dating (Fig. 6c) shows that secondary monazite is Paleoproterozoic and compositionally similar to primary monazite (Fig. 8).

JC-308-03 (pegmatite dike)

Sample 308 is from a 2–4 m wide muscovite biotite pegmatite dike that shows pinch-and-swell; the dike is vertical and cuts the gneissosity in the host gneisses at a high angle (Fig. 4d). It has a weak foliation defined by aligned

coarse biotite that parallels the gently dipping gneissosity in the host gneisses. It contains small lenses of grey medium-grained, weakly foliated biotite granite that is similar to Bourne granite (samples JC-13-03 and JC-19-03).

Zircon is oscillatory-zoned (Fig. 5d) and the U-rich nature is indicated by the CL-dark character that typifies zircon with high U concentrations. Sixteen grains yielded a weighted mean age of 1856 ± 10 Ma (MSWD = 0·7) (Fig. 3d). Cores with different zoning patterns and CL brightness are common, with two having ages of ~1·96 Ga. Monazite has a variety of zoning patterns, including oscillatory, sector, and patchy (Fig. 6d). Ten grains yielded a weighted mean age of $50{\cdot}7 \pm 1{\cdot}8$ Ma (MSWD = 0·6) (Fig. 3d). EPMA dating shows that all monazite is Tertiary (Fig. 6d) and compositionally diverse (Fig. 8). Heterogeneity in the abundance of monazite in the dike is shown by the lack of monazite in a sample previously collected at the same locality (Crowley, 1999).

JC-08-03 (pegmatite dike)

Sample JC-08-03 is from a narrow (0·1–1 m wide) garnet muscovite biotite pegmatite dike that is vertical and cuts the gneissosity in the host gneisses at a high angle (Fig. 4e and f). The igneous textures and undeformed appearance suggest intrusion after gneissosity formation.

Zircon has mostly oscillatory and sector zoning (Fig. 5e). Twenty-four values from 21 grains yielded a weighted mean age of 1845 ± 7 Ma (MSWD = 0·6) (Fig. 3e). Cores with different zoning patterns and CL brightness exist in ~20% of the imaged grains, but none were dated because of small size. Monazite is strongly oscillatory- and sector-zoned (Fig. 6e). Twenty grains yielded a weighted mean age of 1850 ± 17 Ma (MSWD = 0·2) (Fig. 3e). The combined zircon and monazite weighted mean age is 1846 ± 7 Ma (MSWD = 0·4). Oscillatory- and sector-zoned monazite has two similar, yet distinct composition populations (Fig. 8). Many grains have small (a few microns) to large (100 μm) domains that are irregular-shaped, have strong patchy to weak zoning, and cut across oscillatory and sector zoning in the rest of the grains (Fig 7c). These characteristics suggest that the domains formed during secondary growth by recrystallization of primary monazite. EPMA dating shows that most secondary domains are Paleoproterozoic [20 of 21 spots placed in secondary monazite are Paleoproterozoic (Fig. 6e)], yet some grains have a considerable amount of Tertiary secondary monazite (Fig. 7c). Secondary Paleoproterozoic monazite has more compositional variability than primary monazite and some Tertiary monazite is poorer in Y than is Paleoproterozoic monazite (Fig. 7c).

AGE INTERPRETATION

Interpretation of whether igneous crystallization of the granitic rocks occurred at 1·9 Ga or 50 Ma is based on U–(Th)–Pb ages of zircon and monazite, field relationships, and mineral composition and zoning. Each dataset on its own is insufficient for age interpretation, but together they provide solid evidence.

U–(Th)–Pb ages

Age interpretation starts with U–(Th)–Pb ages from all zircon and monazite chemical domains large enough for analysis. Zircon ages are equivalent within each sample, excluding the small number of ages >1·95 Ga from cores and whole grains that appear to be inherited based on differences in zoning and CL brightness. Ages are also equivalent between samples with a weighted mean of 1851 ± 5 Ma (MSWD = 0·8), excluding sample JC-09-03, which yielded a weighted mean of 1925 ± 15 Ma. No younger zircon was found, but it is not certain that all zircon is 1·9 Ga because the 40 μm × 40 μm spot of the laser was too large for dating the narrow rims on some grains. The overwhelming dominance of 1·9 Ga zircon may indicate igneous crystallization at 1·9 Ga. However, evidence other than zircon ages must be considered given the possibility that all zircon is inherited.

Monazite with an age of 1·9 Ga makes up >90% of the population in four samples. The 1·9 Ga monazite ages are equivalent within each sample and between samples with a weighted mean of 1852 ± 8 Ma (MSWD = 0·6). Zircon and monazite ages from all samples are equivalent with a weighted mean of 1851 ± 4 (MSWD = 0·7), excepting the above-mentioned older and younger ages. Monazite with an age of 50 Ma forms all of the population in one sample and <10% of the other samples. The rarity of monazite inheritance and the dominance of 1·9 Ga monazite in four samples suggest that igneous crystallization occurred at 1·9 Ga. However, evidence other than monazite ages must be considered because there is one known case of complete monazite inheritance (Gilotti & McClelland, 2005).

Field relationships

Inheritance can be identified upon comparison of U–Pb ages with relative ages based on field relationships. U–Pb ages must be consistent with relative ages if the granitic rocks crystallized at 1·9 Ga, but not necessarily if 1·9 Ga zircon and monazite are inherited. Pegmatite layer JC-09-03 is considered to be the oldest sample because it was deformed by two fold generations, the earlier of which resulted in isoclinal structures (Fig. 4a); the other samples are weakly deformed or undeformed (Fig. 4b–f). For example, pegmatite dyke JC-08-03 is undeformed and is only 35 m from JC-09-03. JC-09-03 has 1925 ± 15 Ma zircon that is older than the dominant zircon in the other samples, showing that U–Pb ages are consistent with relative ages.

Inheritance is also assessed by comparing the ages of zircon and monazite with those in the host rocks, the likely source for inherited grains in these small-volume,

locally derived granitic rocks. The host rocks are 2·3–2·1 Ga orthogneiss and older paragneiss. Two samples do contain 2·3–2·1 Ga zircon that is thought to be inherited because it occurs as cores and whole grains with different zoning patterns and CL brightness compared with the dominant 1·9 Ga zircon. A similar origin is probable for ~1·98 Ga zircon cores in two samples. A 1·9 Ga gneiss that could be an inheritance source for the dominant 1·9 Ga zircon and monazite is not known in the study area; the nearest dated 1·9 Ga gneiss lies ~30 km to the NW. Nevertheless, evidence other than field relationships must be considered because it cannot be ruled out that 1·9 Ga gneiss exists in the study area given the small number of dated samples, and it may lie below the exposed surface.

Mineral composition and zoning

Several assumptions are made when using the composition and zoning of zircon and monazite to assess inheritance. Grains that formed during igneous crystallization of the sample should have (1) zoning typical of grains crystallized from magma, (2) similar composition and zoning within samples, and (3) different composition and zoning between samples. Inherited grains should be (1) broadly similar to grains in the host rocks, the likely inheritance sources for small-volume, locally derived granitic rocks, and (2) similar between samples. It is expected that inherited grains in our study would have variable composition and zoning within each sample because the granitic rocks are hosted by heterogeneous gneisses. Moreover, most inherited grains should not appear to be from peraluminous granitic magmas given the lack of peraluminous granitic rocks in the host gneisses.

The 1·9 Ga zircon is thought to have formed during igneous crystallization of the sample because CL brightness and zoning are similar within samples and different between samples (Fig. 5). Bright grains in JC-08-03 with strong fine oscillatory zoning contrast with dark grains in JC-09-03 with weak oscillatory zoning. Grains in JC-308-03 are also dark, but differ from those in JC-09-03 by having better developed oscillatory zoning. Grains in JC-13-03 and JC-19-03 have similar strong oscillatory and sector zoning; similarity is expected because these samples are from identical-looking granite sheets that are considered to be part of the Bourne granite suite. Growth of zircon from magma is suggested by the oscillatory and sector zoning (Fig. 5) (Corfu *et al.*, 2003). Growth from granitic magmas is suggested by moderate to high U concentrations that are typical of granitic magmas. The CL-dark nature of zircon in JC-09-03 and JC-308-03 indicates that the grains are U-rich, and ID-TIMS dating shows that zircon in rocks from which JC-08-03 and JC-308-03 were collected are U-rich, with 1000–2200 and 500–2500 ppm, respectively (Crowley, 1999). In contrast, zircon in the host gneisses is poorer in U, with <500 ppm (Crowley, 1999).

The 1·9 Ga monazite is also thought to have formed during igneous crystallization of the sample because of similarities in zoning within samples and differences between samples (Fig. 6). Strong oscillatory zoning in grains in JC-08-03 and JC-19-03 contrasts with patchy zoning in grains in JC-09-03 and sector zoning in grains in JC-13-03. Primary 1·9 Ga monazite is compositionally uniform within samples and rather distinct between samples (Fig. 8), with the exception of the two samples of Bourne granite (JC-13-03 and JC-19-03) that are similar. Monazite growth in JC-08-03 and JC-19-03 from magmas is suggested by oscillatory zoning (Fig. 6).

Sample JC-308-03 differs from the others by containing monazite with drastically different zoning. There is more variability in BSE brightness between grains in JC-308-03 than there is between grains in all other samples (Fig. 9). This observation is important because JC-308-03 is the only sample with only 50 Ma monazite. The 50 Ma monazite is compositionally diverse, with nearly as much diversity within JC-308-03 as between all primary 1·9 Ga monazite in the other four samples (Fig. 8). Based on the inference that metamorphic fluids are more compositionally diverse than granitic magmas, we suggest that the variable zoning and composition in 50 Ma monazite is due to growth from metamorphic fluids. Metamorphic monazite can be oscillatory-zoned, but it typically has patchy zoning. Patchy zoning in JC-09-03 indicates a metamorphic origin for grains that grew ~60 Myr after magmatic zircon in the sample.

Igneous crystallization at 1·9 Ga

We conclude that the granitic rocks crystallized at 1·9 Ga and were metamorphosed at 50 Ma during the Cordilleran orogenesis because 1·9 Ga zircon and monazite inheritance is unlikely given that (1) the host rocks are heterogeneous 2·3–2·0 Ga gneisses; (2) zircon yielded 1·9 Ga ages that are equivalent within samples; (3) zircon is from magma that appears to be unique to each sample; (4) >90% of the monazite in four of five samples yielded 1·9 Ga monazite ages that are equivalent within samples; (5) 1·9 Ga monazite in three samples is from magma that appears to be unique to each sample; (6) variable composition and zoning of 50 Ma monazite suggest growth from metamorphic fluids; (7) field relationships are consistent with 1·9 Ga igneous crystallization.

The crystallization age of the strongly deformed pegmatite layer (JC-09-03) is interpreted from the zircon age of 1925 ± 15 Ma. The 1863 ± 13 Ma monazite grew during metamorphism that coincided with intrusion of the other samples, which were weakly deformed to undeformed. Crystallization ages of weakly deformed Bourne granites, JC-13-03 and JC-19-03, are interpreted from the combined zircon and monazite ages of 1846 ± 14 and 1855 ± 9 Ma, respectively. The crystallization age of the weakly deformed pegmatite dike (JC-308-03) is interpreted from

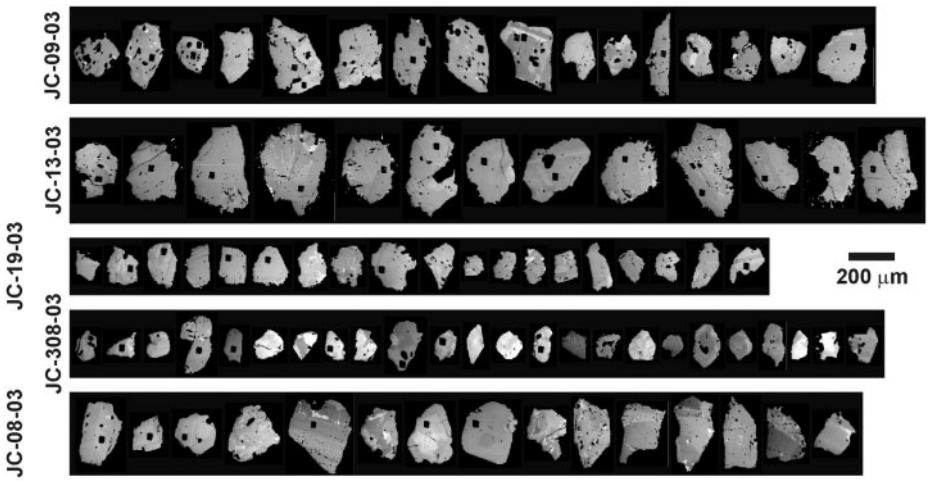

Fig. 9. BSE images of monazite that were collected simultaneously within each sample, showing differences in BSE brightness within samples.

the zircon age of 1856 ± 10 Ma. The 50·7 ± 1·8 Ma monazite grew during Cordilleran metamorphism, synchronous with monazite in nearby pelitic schist (Crowley & Parrish, 1999). The crystallization age of the undeformed pegmatite dike (JC-08-03) is interpreted from the combined zircon and monazite age of 1846 ± 7 Ma.

Results confirm that basement gneisses in a small (several square kilometers) part of the Frenchman Cap dome were last strongly deformed and partly melted at 1·9 Ga (Crowley, 1999; Crowley *et al.*, 2001). If granite that is considered to be part of the Bourne granite suite based on appearance and field relationships is indeed part of the suite, the region that escaped severe Tertiary (Cordilleran) tectonism is considerably larger, perhaps tens of square kilometers. The weak Tertiary overprint experienced by parts of the Frenchman Cap basement contrasts with the intense Tertiary tectonism recorded in higher structural levels of the dome (Journeay, 1986; Crowley & Parrish, 1999; Crowley *et al.*, 2001; Foster *et al.*, 2004) and in many parts of the Thor–Odin dome (Vanderhaeghe *et al.*, 1999; Hinchey *et al.*, 2006, 2007). Further geochronology, petrology, and structural analysis are needed to explain the differences in the intensity of Tertiary tectonism between structural levels within the Frenchman Cap dome and between it and the Thor–Odin dome.

SUMMARY

Identifying inherited zircon and monazite is crucial for accurate geochronology of granitic rocks. U–(Th)–Pb ages from all chemical domains are the starting dataset to which other types of evidence are added. We use zircon and monazite ages, field relationships, and mineral composition and zoning to show that five granitic rocks in the Canadian Cordillera crystallized at 1·9 Ga rather than during Cordilleran orogenesis at 50 Ma. Zircon and monazite yielded 1·9 Ga ages that are equivalent within samples, except for small 50 Ma monazite domains and one sample with only 50 Ma monazite. The oldest sample based on field relationships yields greater ages than the other samples. The granitic rocks are small-volume melts hosted by heterogeneous 2·3–2·0 Ga gneisses lacking 1·9 Ga components that could be the sources for any 1·9 Ga inherited grains. The 1·9 Ga grains have composition and zoning suggestive of crystallization from granitic magmas. These aspects are uniform within samples, yet differ between samples, indicating that the grains crystallized from magmas unique to each sample; this scenario would be fortuitous if the 1·9 Ga grains are inherited. The 50 Ma monazite is compositionally different from the 1·9 Ga monazite and variable within samples, suggesting that it did not grow from a uniform source such as a magma, but from rather diverse metamorphic fluids.

The presence of weakly deformed to undeformed 1·9 Ga sheets and dikes indicates that a structurally deep part of the Cordillera remained free of melt and rigid throughout Tertiary orogenesis.

ACKNOWLEDGEMENTS

Research was supported by the Natural Sciences and Engineering Research Council of Canada Discovery grant to R.L.B. Technical assistance with the LA-ICPMS system was provided by M. Tubrett and assistance with the electron microprobe was provided by N. Chatterjee and M. Jercinovic. We appreciate reviews of the manuscript by P. Dahl, W. McClelland, and C. McFarlane, and careful editing by R. Frost.

SUPPLEMENTARY DATA

Supplementary data for this paper are available at *Journal of Petrology* online.

REFERENCES

Armstrong, J. T. (1995). CITZAF—a package of correction programs for the quantitative electron microbeam X-ray analysis of thick polished materials, thin-films and particle. *Microbeam Analysis* **4**, 177–200.

Armstrong, R. L., Parrish, R. R., van der Heyden, P., Scott, K., Runkle, D. & Brown, R. L. (1991). Early Proterozoic basement exposures in the southern Canadian Cordillera: core gneiss of Frenchman Cap, Unit I of the Grand Forks Gneiss and Vaseaux Formation. *Canadian Journal of Earth Sciences* **28**, 1169–1201.

Bea, F., Montero, P., González-Lodeiro, F. & Talavera, C. (2007). Zircon inheritance reveals exceptionally fast crustal magma generation processes in Central Iberia during the Cambro-Ordovician. *Journal of Petrology* **48**, 2327–2339.

Brown, R. L. & Gibson, H. D. (2006). An argument for channel flow in the southern Canadian Cordillera and comparison with Himalayan tectonics. In: Law, R. D., Searle, M. P. & Godin, L. (eds) *Channel Flow, Ductile Extrusion and Exhumation in Continental Collision Zones. Geological Society, London, Special Publications* **268**, 543–559.

Brown, R. L., Journeay, J. M., Lane, L. S., Murphy, D. C. & Rees, C. J. (1986). Obduction, backfolding and piggyback thrusting in the metamorphic hinterland of the southeastern Canadian Cordillera. *Journal of Structural Geology* **8**, 225–268.

Copeland, P., Parrish, R. R. & Harrison, T. M. (1988). Identification of inherited radiogenic Pb in monazite and its implications for U–Pb systematics. *Nature* **333**, 760–763.

Corfu, F., Hanchar, J. M., Hoskin, P. W. O. & Kinny, P. (2003). Atlas of zircon textures. In: Hanchar, J. M. & Hoskin, P. W. O. (eds) *Zircon. Mineralogical Society of America, Reviews in Mineralogy and Geochemistry* **53**, 468–500.

Crowley, J. L. (1997). U–Pb geochronologic constraints on the cover sequence of the Monashee complex, Canadian Cordillera: Paleoproterozoic deposition on basement. *Canadian Journal of Earth Sciences* **34**, 1008–1022.

Crowley, J. L. (1999). U–Pb geochronologic constraints on Paleoproterozoic tectonism in the Monashee complex, Canadian Cordillera: elucidating an overprinted geologic history. *Geological Society of America Bulletin* **111**, 560–577.

Crowley, J. L. & Parrish, R. R. (1999). U–Pb isotopic constraints on diachronous metamorphism in the northern Monashee complex, southern Canadian Cordillera. *Journal of Metamorphic Geology* **17**, 483–502.

Crowley, J. L., Brown, R. L. & Parrish, R. R. (2001). Diachronous deformation and a strain gradient beneath the Selkirk allochthon, northern Monashee complex, southeastern Canadian Cordillera. *Journal of Structural Geology* **23**, 1103–1121.

Crowley, J. L., Myers, J. S., Sylvester, P. J. & Cox, R. A. (2005). Detrital zircon from the Jack Hills and Mount Narryer, Western Australia: evidence for diverse >4·0 Ga source rocks. *Journal of Geology* **113**, 239–263.

Foster, G., Parrish, R. R., Horstwood, M. S. A, Chenery, S., Pyle, J. & Gibson, H. D. (2004). The generation of prograde *P–T–t* points and paths; a textural, compositional, and chronological study of metamorphic monazite. *Earth and Planetary Science Letters* **228**, 125–142.

Gilotti, J. A. & McClelland, W. C. (2005). Leucogranites and the time of extension in the East Greenland Caledonides. *Journal of Geology* **113**, 339–417.

Goncalves, P., Williams, M. L. & Jercinovic, M. J. (2005). Electron-microprobe age mapping of monazite. *American Mineralogist* **90**, 578–585.

Harrison, T. M., Aleinikoff, J.N. & Compston, W. (1987). Observations and controls on the occurrence of inherited zircon in Concord-type granitoids, New Hampshire. *Geochimica et Cosmochimica Acta* **5**, 2549–2558.

Harrison, T. M., McKeegan, K. D. & Le Fort, P. (1995). Detection of inherited monazite in the Manaslu leucogranite by $^{208}Pb/^{232}Th$ ion microprobe dating: crystallization ages and tectonic implications. *Earth and Planetary Science Letters* **133**, 271–282.

Harrison, T. M., Catlos, E. J. & Montel, J. M. (2002). U–Th–Pb dating of phosphate minerals. In: Kohn, M. J., Rakovan, J. & Hughes, J. M. (eds) *Phosphates: Geochemical, Geobiological, and Materials Importance. Mineralogical Society of America, Reviews in Mineralogy and Geochemistry* **48**, 523–558.

Hinchey, A. M., Carr, S. D., McNeill, P. & Rayner, N. (2006). Paleocene–Eocene high-grade metamorphism, anatexis, and deformation in the Thor–Odin dome, Monashee complex, southeastern British Columbia. *Canadian Journal of Earth Sciences* **43**, 1341–1365.

Hinchey, A. M., Carr, S. D. & Rayner, N. (2007). Bulk compositional controls on the preservation of age domains within metamorphic monazite: A case study from quartzite and garnet–cordierite–gedrite gneiss of Thor–Odin dome, Monashee complex, Canadian Cordillera. *Chemical Geology* **240**, 85–102.

Jackson, S. E., Longerich, H. P., Dunning, G. R. & Fryer, B. J. (1992). The application of laser-ablation microprobe: inductively coupled plasma-mass spectrometry (LAM-ICP-MS) to *in situ* trace-element determinations in minerals. *Canadian Mineralogist* **30**, 1049–1064.

Johnston, D. H., Williams, P. F., Brown, R. L., Crowley, J. L. & Carr, S. D. (2000). Northeastward extrusion and extensional exhumation of crystalline rocks from the Monashee complex, southeastern Canadian Cordillera. *Journal of Structural Geology* **22**, 603–625.

Journeay, J. M. (1986). Stratigraphy, internal strain, and thermo-tectonic evolution of northern Frenchman Cap dome, an exhumed basement duplex structure, Omineca hinterland, southeastern Canadian Cordillera. PhD dissertation, Queen's University, Kingston, Ontario..

Košler, J. & Sylvester, P. S. (2003). Present trends and the future of zircon in geochronology: laser ablation ICPMS. In: Hanchar, J. M. & Hoskin, P. W. O. (eds) *Zircon. Mineralogical Society of America, Reviews in Mineralogy and Geochemistry* **53**, 243–275.

Ludwig, K. A. (2003). *Isoplot/Ex ver. 3.00, A geochronological tool kit for Microsoft Excel. Berkeley Geochronology Center Special Publications* **4**.

Miller, C. F., Hatcher, R. D., Ayers, J. C., Coath, C. D. & Harrison, T. M. (2000). Age and zircon inheritance of eastern Blue Ridge plutons, southwestern North Carolina and northeastern Georgia, with implications for magma history and evolution of the southern Appalachian orogen. *American Journal of Sciences* **300**, 142–172.

Mojzsis, S. J. & Harrison, T. M. (2002). Establishment of a 3·83-Ga magmatic age for Akilia tonalite (southern West Greenland). *Earth and Planetary Science Letters* **202**, 563–576.

Montel, J. M. (1993). A model for monazite/melt equilibrium and application to the generation of granitic magmas. *Chemical Geology* **110**, 127–146.

Nutman, A. P., Mojzsis, S. J. & Friend, C. R. (1997). Recognition of >3850 Ma water-lain sediments in West Greenland and their significance for the early Archaean Earth. *Geochimica et Cosmochimica Acta* **61**, 2475–2484.

Parkinson, D. (1991). Age and isotopic character of Paleoproterozoic basement gneisses in the southern Monashee complex, southeastern British Columbia. *Canadian Journal of Earth Sciences* **28**, 1159–1168.

Parrish, R. R. (1995). Thermal evolution of the southeastern Canadian Cordillera. *Canadian Journal of Earth Sciences* **32**, 1618–1642.

Parrish, R. R. & Noble, S. R. (2003). Zircon U–Th–Pb geochronology by isotope dilution-thermal ionization mass spectrometry (ID-TIMS). In: Hanchar, J. M. & Hoskin, P. W. O. (eds) *Zircon. Mineralogical Society of America, Reviews in Mineralogy and Geochemistry* **53**, 183–213.

Pyle, J. M., Spear, F. S. & Wark, D. A. (2002). Electron microprobe analysis of REE in apatite, monazite, and xenotime: protocols and pitfalls. In: Kohn, M. J., Rakovan, J. & Hughes, J. M. (eds) *Phosphates: Geochemical, Geobiological, and Materials Importance. Mineralogical Society of America, Reviews in Mineralogy and Geochemistry* **48**, 337–362.

Rapp, R. P., Ryerson, F. J. & Miller, C. F. (1987). Experimental evidence bearing on the stability of monazite during crustal anatexis. *Geophysical Research Letters* **14**, 307–310.

Roddick, J. C. & Bevier, M. L. (1995). U–Pb dating of granites with inherited zircon: conventional and ion microprobe results from two Paleozoic plutons, Canadian Appalachians. *Chemical Geology* **119**, 307–329.

Teyssier, C., Ferré, E., Whitney, D. L., Norlander, B., Vanderhaeghe, O. & Parkinson, D. (2005). Flow of partially molten crust and origin of detachments during collapse of the Cordilleran orogen. In: Bruhn, D. & Burlini, L. (eds) *High-strain Zones: Structures and Physical Properties. Geological Society, London, Special Publications* **245**, 39–64.

Vanderhaeghe, O., Teyssier, C. & Wysoczanski, R. (1999). Structural and geochronological constraints on the role of partial melting during the formation of the Shuswap metamorphic core complex at the latitude of the Thor–Odin dome, British Columbia. *Canadian Journal of Earth Sciences* **36**, 917–943.

Watson, E. B. & Harrison, T. M. (1983). Zircon saturation revisited: temperature and composition effects in a variety of crustal magma types. *Earth and Planetary Science Letters* **64**, 295–304.

Wheeler, J. O. (1965). Big Bend map-area, British Columbia. Geological Survey of Canada. Paper 64–32.

Wheeler, J. O., McFeely, & P. (compilers), (1991). Tectonic assemblage map of the Canadian Cordillera and adjacent parts of the United States of America, scale 1:2,000,000. *Geological Survey of Canada Map* 1712A.

Whitehouse, M. J., Kamber, B. S. & Moorbath, S. (1999). Age significance of U–Th–Pb zircon data from early Archaean rocks of west Greenland—a reassessment based on combined ion-microprobe and imaging studies. *Chemical Geology* **160**, 201–224.

Wiedenbeck, M., Alle, P., Corfu, F., Griffin, W. L., Meier, M., Oberli, F., von Quadt, A., Roddick, J. C. & Spiegel, W. (1995). Three natural zircon standards for U–Th–Pb, Lu–Hf, trace element, and REE analyses. *Geostandards Newsletter* **19**, 1–23.

Williams, P. F. & Jiang, D. (2005). An investigation of lower crustal deformation: Evidence for channel flow and its implications for tectonics and structural studies. *Journal of Structural Geology* **27**, 1486–1504.